Synthesis and optical properties of the Eu^{2+}-doped alkaline-earth metal hydride chlorides $AE_7H_{12}Cl_2$ (AE = Ca and Sr)

Daniel Rudolph[a], Thomas Wylezich[b], Atul D. Sontakke[c], Andries Meijerink[c], Philippe Goldner[d], Philip Netzsch[e], Henning A. Höppe[e], Nathalie Kunkel[b,*], Thomas Schleid[a,**]

[a] *University of Stuttgart, Institute for Inorganic Chemistry, Pfaffenwaldring 55, 70569 Stuttgart, Germany*
[b] *Technical University of Munich, Chair for Inorganic Chemistry with Focus on Novel Materials, Lichtenbergstr. 4, 85748 Garching, Germany*
[c] *Utrecht University, Debye Institute, P.O. Box 80 000, 3508 TA Utrecht, the Netherlands*
[d] *PSL University, Chimie ParisTech, CNRS, Institut de Recherche de Chimie Paris, 75005 Paris, France*
[e] *Universität Augsburg, Institut für Physik, Universitätsstr. 1, D-86159 Augsburg, Germany*

A R T I C L E I N F O

A B S T R A C T

In our study of the optical properties of Eu^{2+}-doped alkaline-earth metal hydride chlorides $AE_7H_{12}Cl_2$ (AE = Ca and Sr) we observe yellow (AE = Sr) and orange-red (AE = Ca) emission. Compared to the emission energies of Eu^{2+}-doped fluorides, chlorides and mixed fluoride chlorides, this corresponds to a wide redshift of the Eu^{2+} $4f^65d^1$–$4f^7$ emission. We explain this observation with the strong polarizability of the hydride anion and therefore its strong nephelauxetic effect, which shifts the 5d barycenter to lower energy. Furthermore, the redshift is even significant compared to other known hydride chlorides and hydride oxide chlorides, which is probably caused by the relatively short $AE^{2+}/Eu^{2+}-H^-$ distances, or it might also be caused by impurity-trapped exciton states. We have also investigated the temperature dependence of the photoluminescence life-times and the thermal stability. Even though the compounds are probably not ideal for phosphor application due to their low stability against air and moisture, our study underlines the large influence of the highly polarizable hydride anion on the optical properties of divalent europium and shows that Eu^{2+} could be used as a probe in mixed anionic systems to determine the hydride content.

1. Introduction

The crystal chemistry and properties of alkaline-earth metal fluoride halides, which crystallize with the PbFCl-type structure, have been investigated elaborately during the course of many years [1–4]. Especially the BaFX:Eu^{2+} series (X = Cl, Br, I) has received a lot of attention, since it can be used as storage phosphor in image plates for X-ray and neutron detectors [5–7]. A large number of investigations on its luminescence properties and, most of all, possible storage mechanisms have been carried out [8–10]. But not only pure halides are known in these systems. In the attempt to synthesize subhalides of the alkaline-earth metals, such as the so-called calcium monochloride [11], Ehrlich et al. discovered the hydride halides [12–14] and later, also the corresponding hydride halides of some divalent rare-earth metal ions were found [15,16]. These hydride halides MHX (M = Ca, Sr, Ba, Eu, Yb, Sm; X = Cl, Br, I) have since then been thoroughly characterized [17] and additionally, a number of further compounds in the phase diagram

MH_2–MX_2 (M = Ca, Sr, Ba, Eu; X = Cl, Br, I), such as Ca$_7$H$_{12}$Cl$_2$ [18], Ca$_2$H$_3$Br [18], Sr$_7$H$_{12}X_2$ (X = Cl, Br) [19], Sr$_2$H$_3$I [20], Ba$_2$H$_3X$ (X = Cl, Br, I) [21,22] or Eu$_2$H$_3$Cl [23] have been discovered. While many optical investigations on fluoride halides doped with rare-earth metal cations have been carried out, the corresponding hydrides have received little attention. The only luminescence studies on hydride chlorides so far have been reported for EuHCl [24] and LiEu$_2$HOCl$_2$ [25]. Yet, luminescence spectroscopy of rare-earth metal ions showing $4f-5d$ transitions can reveal important information regarding the polarizability of the surrounding anions. This is because the 5d levels are not shielded but fully exposed to the orbitals of the ligands, so that both, the crystal field splitting as well as the nephelauxetic effect, play an important role. For instance, Eu^{2+} ions doped into nitridosilicates show a significant redshift of the barycenter of the 5d levels and the emission energies [26,27] compared to less polarizable anions [28]. Another anion with a high polarizability is hydride. Lately, photoluminescence [29,30] and thermoluminescence [31] in Eu^{2+}-doped

hydrides have been studied and it was found that the high polarizability leads to an extreme redshift of the barycenter of the 5d levels. As a consequence, it is possible to vary the emission energy by variation of the hydride content in mixed-anionic hydride fluorides [32–34], which then corresponds to tuning the polarizability of the chemical environment. It can therefore be expected that the Eu^{2+} emission energies in the hydride halides will show a redshift compared to the fluoride halides. Here, we study the Eu^{2+} luminescence in the doped hydride chlorides $Ca_7H_{12}Cl_2:Eu^{2+}$ and $Sr_7H_{12}Cl_2:Eu^{2+}$.

2. Experimental section

2.1. Synthesis

Due to their moisture and air sensitivity, the starting materials and products were handled in an argon-filled glovebox (GS Glovebox Systemtechnik). To ensure a homogeneous distribution of europium atoms in the alkaline-earth metal (w(Eu) = 0.5 mol-%), pieces of europium (Eu: 99.9%, ChemPur) and the respective alkaline-earth metal (Ca: 99.98%, Sr: 99%, both Alfa-Aesar) were fused several times by arc-welding the metals under argon in the glovebox. For the calcium compound, 165 mg of the calcium-europium mixture reacted with 46 mg of sodium amide (Na[NH₂]: self-made), 63 mg sodium chloride (NaCl: 99.99%, Merck) using 130 mg of sodium (Na: ACS grade, Alfa Aesar) as a flux. To obtain the strontium compound, 211 mg of the strontium-europium mixture and 47 mg of ammonium chloride ([NH₄]Cl: for analysis, Merck), strontium chloride (SrCl₂: 99.99%, Alfa Aesar) and sodium each were used. After transferring the reactants into niobium capsules, which were cleaned prior to use in a mixture of sulfuric, nitric and hydrofluoric acid, they were arc-welded under helium. To prevent their oxidation, the niobium capsules were enclosed into evacuated silica ampoules and tempered in a muffle furnace at 900 °C for 24 ($Ca_7H_{12}Cl_2$) or 12 h ($Sr_7H_{12}Cl_2$). While up to 2 mm long crystals of the strontium compound were obtained without a special cooling procedure by just switching off the furnace, the calcium compound only formed in sufficiently large crystals after cooling down within 72 h to room temperature.

Since sodium was used as a flux, it had to be removed by dissolving it in liquid ammonia using a tensi-eudiometer [35]. The opened niobium capsule was placed in an H-shaped glass tube that could be connected via a flange to the tensi-eudiometer, which was filled with gaseous ammonia after evacuating. By using an ethanol-dry ice cooling bath liquid ammonia could be condensed into the H-shaped tube and the sodium dissolved. Afterwards, the dark blue sodium solution was poured into the second leg of the H-shaped tube by holding it horizontally. By gentle heating of the sodium solution, the ammonia evaporated and the whole procedure was repeated, until the liquid ammonia merely showed a faint blue color. After evacuating the tube again, it could be brought into the glove box, where crystals of the hydride chlorides could be selected for single-crystal X-ray diffraction and the luminescence measurements.

2.2. Characterization

2.2.1. Single-crystal X-ray diffraction

For both compounds, $Ca_7H_{12}Cl_2:Eu^{2+}$ and $Sr_7H_{12}Cl_2:Eu^{2+}$, several single crystals were selected under a light microscope (M60, Leica Microsystems) in the glove box and put into thin-walled glass capillaries (Hilgenberg) with a diameter of 0.1 mm. The so prepared single crystals could be used to determine unit-cell parameters on a κ-CCD diffractometer (Bruker-Nonius) in order to verify the successful synthesis of the desired alkaline-earth metal hydride chlorides.

2.2.2. Optical measurements

Due to air and moisture sensitivity, the crystals were enclosed into silica ampoules with 5 mm diameter for all optical measurements.

Photoluminescence spectra were recorded with a tunable optical parametric oscillator pumped by a neodymium-YAG laser (Ekspla NT342B-SH with 6 ns pulse lengths) together with a Jobin-Yvon HR250 monochromator (600 grooves/mm) and a PI-MAX ICCD camera (Princeton Instruments) for detection. Samples were excited at 365 nm. To increase the signal-to-noise ratio, 100 accumulations were collected per measurement. For temperature dependent measurements, the samples were placed into a Janis closed-cycle helium cryostat with a Lakeshore temperature controller. Samples were fixed to the cold finger using high purity silver paint and copper foil. Decay measurements were recorded on the same set-up. Data were recorded 50 ns after the laser pulse and up to 5 µs delays with an integration window of 20 ns. Photoluminescence excitation spectra at room temperature were recorded using a Xe plasma lamp (Energetic EQ99X) with a Jobin-Yvon HR 250 monochromator (1200 grooves/mm) for excitation and an Acton Spectra Pro 2150 Dual Grating Monochromator together with a Pixis 100 CCD camera for emission. All spectra were corrected for lamp intensity. Further photoluminescence and thermoluminescence measurements were carried out on a Edinburgh Instrument FLS920 spectrofluorometer equipped with a double monochromator for the excitation beam (Czerny-Turner, 300 mm focal length) and a monochromator for UV/Vis detection. The sample was excited with a 450 W Xenon lamp and a Hamamatsu R928 photomultiplier tube (PMT) was used for the emission signal detection. For thermoluminescnce, the samples were cooled down to 4 K, irradiated with 365 nm Hg lamp for three minutes and then the thermoluminescece was investigated in the temperature range from 4 K to 297 K. Low temperature measurements were carried out in an Oxford Instruments liquid helium flow cryostat.

3. Results and discussion

3.1. Crystal structure

The crystal structure of both hydride chlorides $AE_7H_{12}Cl_2$ (AE = Ca and Sr) was already described in Refs. [18,19] and is isostructural to the ordered variant of the barium fluoride chloride $Ba_7F_{12}Cl_2$ in the space group $P\bar{6}$ [36], where also the structural model for the hydride compounds was taken from because no accurate positions for the hydride anions in $AE_7H_{12}Cl_2$ representatives exist due to the lack of neutron diffraction studies. Since the coordination spheres of the three crystallographically different alkaline-earth metal cations by the anions are important for the luminescence studies, they will briefly be discussed here. All three AE^{2+} cations are surrounded by nine anions forming tricapped trigonal prisms. While $(AE1)^{2+}$ is solely coordinated by hydride anions, the coordination spheres of $(AE2)^{2+}$ and $(AE3)^{2+}$ are built up by seven H⁻ and two Cl⁻ anions (Fig. 1).
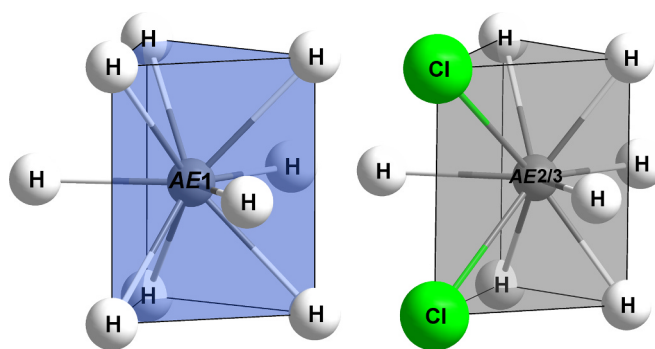

Fig. 1. Coordination polyhedra $[(AE1)H_9]^{7-}$ (left) and $[(AE2/AE3)H_7Cl_2]^{7-}$ (right) in the crystal structure of the hydride chlorides $AE_7H_{12}Cl_2$ (AE = Ca and Sr).
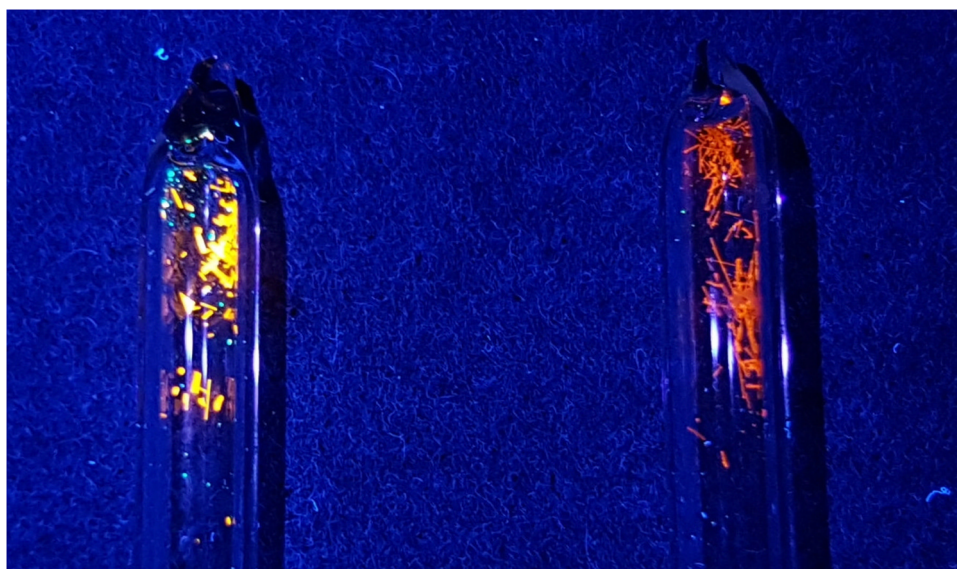
Fig. 2. Single crystals of $Sr_7H_{12}Cl_2:Eu^{2+}$ (left) and $Ca_7H_{12}Cl_2:Eu^{2+}$ (right) under UV light.

3.2. Photoluminescence and absorption

Under UV excitation, $Sr_7H_{12}Cl_2:Eu^{2+}$ shows a bright yellow emission, while the emission of $Ca_7H_{12}Cl_2:Eu^{2+}$ is rather orange-red (Fig. 2). At room temperature, $Sr_7H_{12}Cl_2:Eu^{2+}$ shows a broad band emission with a maximum at 595 nm (Fig. 3a), which is assigned to the Eu^{2+} $4f^65d^1$–$4f^7$ transition. At low temperatures, higher intensities are observed and the maximum is slightly shifted to lower wavenumbers. From about 125 K onwards, the intensities decrease significantly with increasing temperature. The broad band emission is due to the existence of two types of cation sites in the crystal structure, the two similar cation sites with a coordination by seven hydride and two chloride anions and the third cation site coordinated exclusively by nine hydride anions. It can be expected that the emission from the site coordinated exclusively by hydride anions is redshifted compared to the sites coordinated by seven hydride and two chloride anions. This is because the impact of the high polarizability of the hydride ligand is expected to be large [29].

The reason for the slight blueshift with increasing temperature is probably the existence of the different lattice sites and their possible different temperature-dependent behavior. In former studies on Eu^{2+} in hydridic materials [29] it was shown that the mechanism of thermal luminescence quenching is likely to be thermally activated photoionization. Here, the emitting $4f^65d^1$ excited state is located just below the conduction band. The emission is then quenched by thermally activated ionization from the excited state to the conduction band. This model is in good agreement with the rather small band gap of hydrides [37] compared to halides or oxides. Assuming that thermal quenching occurs at slightly lower temperatures for the cation site surrounded by nine hydride anions, this might also explain why the peak maximum of the broad band emission is located at 605 nm at low temperatures and shifts to 595 nm at higher temperatures. The observed broad band emission can be considered an envelope curve comprising the emission peaks of both cation sites, which are too close to each other to be clearly separated. If the intensity of the lower energy emission maximum decreases faster with increasing temperatures than the higher energy emission maximum, this will lead to an apparent blueshift of the total emission band. Deconvoluted emission curves and further luminescence spectra can be found in Fig. S1 in the Electronic Supporting Information.

Another possible explanation is the presence of impurity-ascribed exciton states. Dorenbos suggests that such a blue-shift, as it is observed for e. g. $CsCaF_3:Eu^{2+}$ and $KCaF_3:Eu^{2+}$ [38], is accomplished by thermal activation from the impurity-trapped exciton state to the 5d state [39]. Eu^{2+} might be oxidized to Eu^{3+} with a trapped electron in the surrounding or other defects might be present. In NaCl-type alkali-metal halides [40] and alkaline-earth metal fluoride halides [41,42] different types of defects, such as F-centers (electrons trapped at halide-ion vacancies), Frenkel defects on the larger halide lattice site, or self-trapped holes have been observed and modelled. In BaFCl anionic conduction
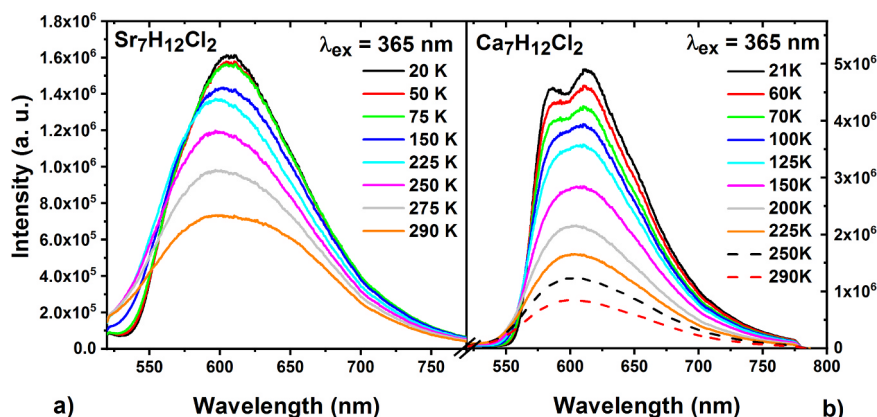

Fig. 3. Temperature-dependent photoluminescence emission spectra of a) Eu^{2+}-doped $Sr_7H_{12}Cl_2$ (0.6 mol-% Eu^{2+}) and b) $Ca_7H_{12}Cl_2$ (0.6 mol-% Eu^{2+}).

via halide vacancies was observed and it was clarified that thermally generated lattice defects are of Schottky type [43]. For ionic hydrides, little is known about defect formation, but considering the so-called hydride-fluoride analogy [44,45] of these compounds, it may be suggested that similar defects also occur in hydrides. Possible defects might, for example, be an electron trapped on anion vacancies or hydride anions on chloride sites. However, thermoluminescence measurements in the range between 4 K and room temperature did not show any thermoluminescence emission. This may either be explained by the absence of glow peaks or because only small amounts of small single crystal samples were available.

In Fig. 3b, the temperature-dependent photoluminescence spectra of Eu^{2+} in the corresponding calcium hydride chloride are shown. As in the case of the strontium compound, a very broad band with a maximum at 600 nm is observed at room temperature. Similar to the strontium compound, the Eu^{2+} emission peaks from the two different lattice sites are not clearly separated. The intensities increase with decreasing temperature. In contrast to the strontium compound, these two emission peaks start to be separated at very low temperatures. Starting from 70 K, it is possible to clearly distinguish between two apparent peak maxima at 590 and 615 nm. Similar to the strontium compound, the peak at lower energy is more intense at low temperatures, but its intensity decreases faster with increasing temperatures. As already discussed for the strontium compound, the two emission peaks are assigned to the two different local environments, two similar sites coordinated by seven hydride and two chloride anions and a third site coordinated exclusively by hydride anions. The observation of several emission peaks is not unexpected, as a similar behavior of the luminescence emission spectra is also found for Eu^{2+}-doped $Ba_7F_{12}Cl_2$ [46,47]. In case of the fluoride chloride, the overlaying emission maxima lead to the total impression of a white-emitting phosphor.

The excitation spectra measured at room temperature for different emission wavelengths (570, 600, and 650 nm) are shown in the Fig. 4a and b. While the excitation spectra of Eu^{2+}-doped $Ba_7F_{12}Cl_2$ [46,47] differ significantly for the different emission wavelengths, the excitation spectra of the hydride chlorides do not show such marked differences. The intensities slightly differ, but the peak positions still remain the same. Both compounds show a maximum at 350 nm in their excitation spectra, with small shoulder at 275 nm and another one at 400 nm.

In the Fig. 5a and b, the temperature-dependent decay curves are depicted for Eu^{2+} in $Sr_7H_{12}Cl_2$ and $Ca_7H_{12}Cl_2$. At low temperatures, the decays show only a slight deviation from single exponential behavior.

With increasing temperature, the lifetimes become significantly shorter and the deviation from a single exponential decay appears larger. For the Eu^{2+} emission in $Sr_7H_{12}Cl_2$ a lifetime of 780 ns is found. The lifetimes become significantly shorter starting from 125 K and at room temperature, 590 ns is finally found (Fig. 6).

The lifetime of the Eu^{2+} emission in $Ca_7H_{12}Cl_2$ at low temperatures is 645 ns. Above 125 K it decreases rapidly and reaches 400 ns at room temperature. These values are in the range of the lifetimes found for the parity-allowed $4f^6 5d^1$–$4f^7$ ($^8S_{7/2}$) emission of divalent europium in hydrides [29,48] and somewhat shorter than in other classes of materials emitting at comparable energies [49]. A possible explanation is the high refractive index n of hydride compounds [50] compared to other materials such as fluorides or oxides [51]. It is well known that the refractive index has a strong influence on the radiative decay rate [52,53]. Many studies on this dependence have already been carried out, for example on the changes in the radiative lifetime of 4f–4f emissions upon changing the particle sizes [54], which corresponds to a change in the refractive index, or on local field effects influencing the radiative lifetime of the 5d–4f emission of Ce^{3+} in different hosts [55]. An increase in the refractive index of the system will lead to a faster radiative decay rate, which is consistent with the observed shorter lifetimes for Eu^{2+} emissions in hydride chlorides. The deviation from single-exponential behavior may be due to the different lattice sites with different thermal quenching behavior. Additionally, the presence of defects influencing the optical properties cannot be completely excluded, but seems unlikely, since no thermoluminescence glow peaks were observed.

In the Figs. 6 and 7, the temperature dependence of the integrated intensities and the lifetime of the Eu^{2+} emission in $Sr_7H_{12}Cl_2$ and $Ca_7H_{12}Cl_2$ are shown. The decrease of the intensities and lifetimes with increasing temperature can be clearly seen, however, a determination of the exact quenching temperature is hampered, since the different emission peaks of the three different lattice sites cannot clearly be separated from each other.

For comparison, Table 1 compiles the emission maxima of different hydride compounds together with the coordination numbers of the Eu^{2+} cations and the Eu–H distances. It can be seen that the emission maxima shift to longer wavelengths for decreasing coordination numbers of the Eu^{2+} cations and also for decreasing Eu–H bond lengths, which is for example true for calcium compared with strontium compounds. It can easily be explained by the smaller ionic radius of Ca^{2+} compared to the heavier alkaline-earth metal cations and therefore smaller unit-cell parameters. These effects lead to a larger ligand-field splitting, which causes a smaller energy gap between the lowest 5d excited state $[Xe]4f^6 5d^1$ of Eu^{2+} and the $4f^7$ ($^8S_{7/2}$) ground state [57]. Due to the strong nephelauxetic effect of the hydride ligand [29], which leads to a lowering of the barycenter of the 5d orbitals [58], the hydride-rich hydride chlorides $AE_7H_{12}Cl_2$ (AE = Ca and Sr) and the pure alkaline-earth metal hydrides AEH_2 with comparably small coordination numbers and Eu–H distances show the most redshifted Eu^{2+} emissions for all hydrides that have so far been investigated. Compared to fluorides, chlorides and fluoride chlorides, the redshift observed in the Eu^{2+} emission is remarkable [57]. For instance, SrFCl:Eu^{2+} shows

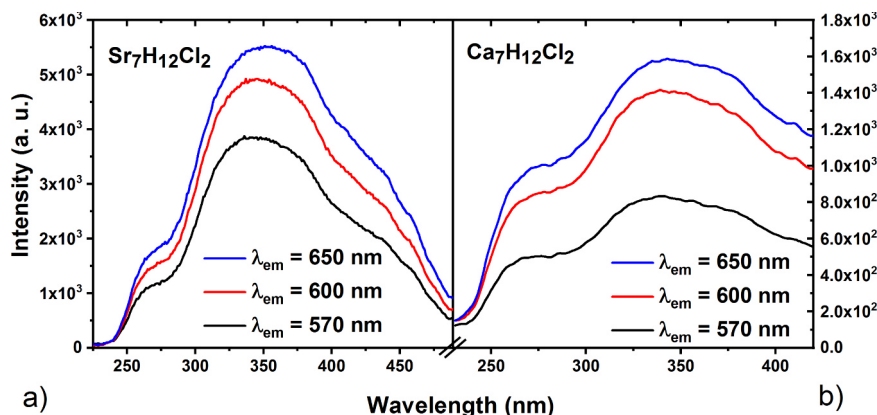**Fig. 4.** Room-temperature photoluminescence excitation spectra of a) $Sr_7H_{12}Cl_2$:Eu^{2+} (0.6 mol-% Eu^{2+}) and b) $Ca_7H_{12}Cl_2$:Eu^{2+} (0.6 mol-% Eu^{2+}).
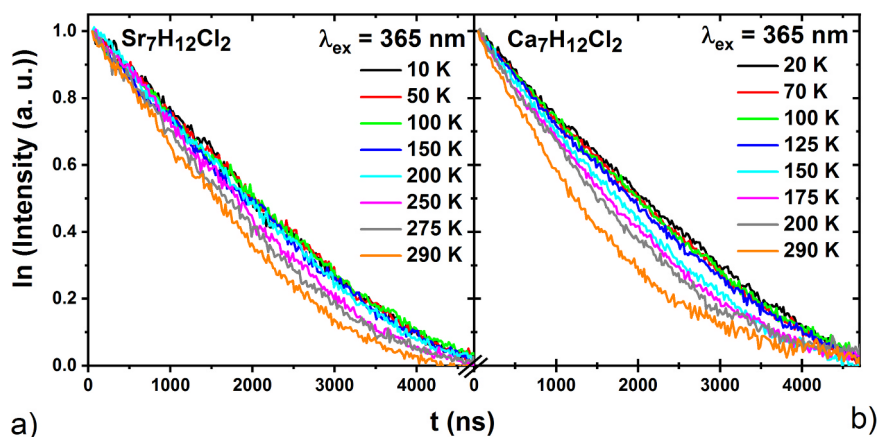
Fig. 5. Temperature-dependent decay curves of a) Eu^{2+}-doped $Sr_7H_{12}Cl_2$ (0.6 mol-% Eu^{2+}) and $Ca_7H_{12}Cl_2$ (0.6 mol-% Eu^{2+}).

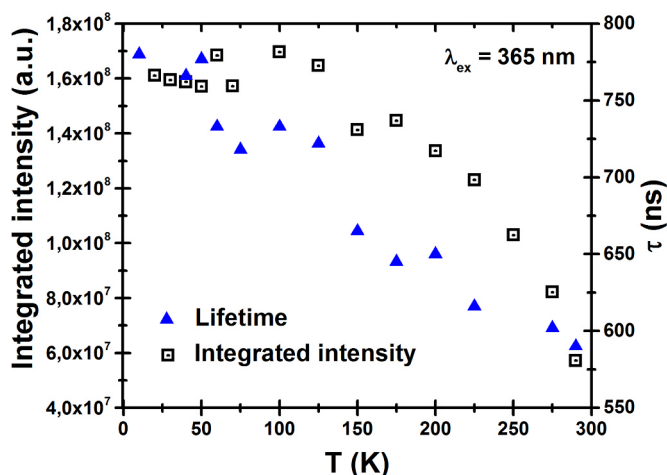**Fig. 6.** Temperature dependence of the integrated photoluminescence emission intensities and the decay times of Eu^{2+}-doped $Sr_7H_{12}Cl_2$ (0.6 mol-% Eu^{2+}).
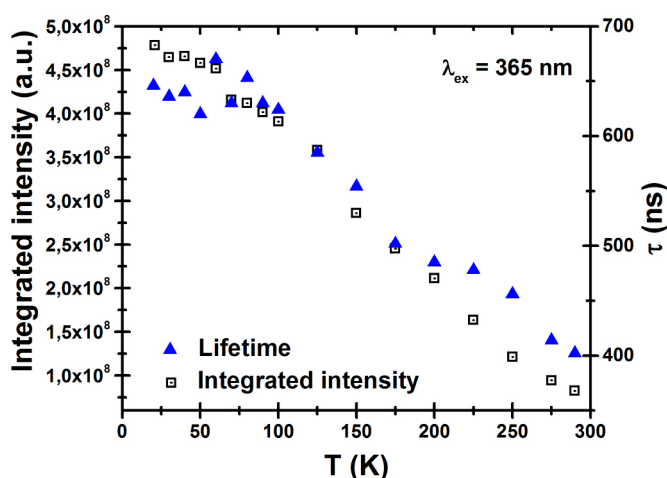

Fig. 7. Temperature dependence of the integrated photoluminescence emission intensities and the decay times of Eu^{2+}-doped $Ca_7H_{12}Cl_2$ (0.6 mol-% Eu^{2+}).

an emission at 388 nm [57,59] and CaFCl:Eu^{2+} at 396 nm [57,60,61]. Also, the Eu^{2+}-doped pure chlorides and fluorides of strontium and calcium emit in the UV-blue color region [59]. A more detailed overview on the so far investigated rare-earth metal ion–doped hydrides and mixed anionic hydrides can be found in Ref. [62].

Table 1

Comparison of the maximum emission wavelengths, the coordination number (CN) of Eu^{2+} and the metal-hydride bond lengths d(Eu–H) in selected hydride compounds.

Compound		$\lambda_{em,\ max}$/nm	$CN(Eu^{2+})$	d(Eu–H)/pm (average)
Eu_2H_3Cl	[23,56]	503	10	240–277 (256)
$KMgHF_2$[a]	[33]	505	12	282
EuHCl	[24]	515	9	248
$KMgH_3$[a]	[48]	565	12	285
$LiSrH_3$:Eu^{2+}	[29]	570	12	271
EuH_xF_{2-x}	[32]	570–685	8	253
$LiEu_2HOCl_2$	[25]	581	9	261–273 (267)
$Sr_7H_{12}Cl_2$	[this work]	595	9	224–284 (257)
$Ca_7H_{12}Cl_2$	[this work]	600	9	223–257 (242)
$SrH_{0.5}F_{1.5}$	[33]	600	8	252
SrH_2	[37]	728	9	243–284 (260)
CaH_2	[37]	764	9	205–270 (234)
$Eu_5H_2O_{2I4}$	[56]	463	8	245, 249 (247)
EuHBr	[56]	493	9	250

[a] Eu^{2+} presumably on the position of K^+.

4. Conclusions

In summary, we have studied Eu^{2+} photoluminescence in the Eu^{2+}-doped hydride chlorides $AE_7H_{12}Cl_2$ (AE = Ca and Sr) and observed yellow (AE = Sr) and orange-red (AE = Ca) emission. This corresponds to a stronger redshift compared to emission energies usually observed for Eu^{2+}-doped fluorides, chlorides and fluoride chlorides, and even compared to several other hydride chlorides and hydride oxide chlorides. We explain this astonishing observation with the high polarizability of the hydride anion and therefore a strong nephelauxetic effect, which shifts the 5d barycenter to lower energy. Furthermore, the AE^{2+}/Eu^{2+}–H^- distances are comparably small, which is also expected to lead to a large crystal field splitting. Consequently, our study confirms the large influence of the highly polarizable hydride anion on the emission energies of divalent europium. Thus, it might also be interesting to study mixed hydride fluoride chlorides, such as $AE_7H_{12-x}F_xCl_2$ in order to tune the emission properties in the future. Even though pure hydrides are not expected to be very air- and thermally stable, Eu^{2+} luminescence might also be used to determine the hydride content in such mixed anionic systems and it is possible that some systems with low hydride content show a higher stability. Especially some hydride oxides ("oxyhydrides") are not sensitive against air- and moisture. With regard to the use of comparable fluoride chlorides as storage phosphors and possible defect formation, it might be worthwhile to also carry out further thermoluminescence studies in these hydride chloride systems. Such studies – as already done for nitridosilicates [26] – might yield helpful information on so far little

studied defect formation mechanisms in hydrides.

Appendix A. Supporting information

Supplementary data associated with this article can be found in the online version at doi:10.1016/j.jlumin.2019.01.033.

References

[1] M. Sauvage, Acta Crystallogr. B 30 (1974) 2786–2787.
[2] V.G. Lambrecht jr.., M. Robbins, R.C. Sherwood, J. Solid State Chem. 10 (1974) 1–4.
[3] H.P. Beck, J. Solid State Chem. 17 (1976) 275–282.
[4] H.P. Beck, Z. Anorg. Allg. Chem. 451 (1979) 73–81.
[5] Y. Amemiya, J. Miyahara, Nature 336 (1988) 89–90.
[6] N. Niimura, Y. Karasawa, I. Tanaka, J. Miyahara, K. Takahashi, H. Saito, S. Koizumi, M. Hidaka, Nucl. Instrum. Methods A 349 (1994) 521–525.
[7] K. Takahashi, J. Lumin. 160 (2002) 307–315.
[8] K. Takahashi, K. Kohda, J. Miyahara, Y. Kanecitsu, K. Amitani, S. Shionaya, J. Lumin. 31–32 (1984) 266–268.
[9] H. von Seggern, T. Voight, W. Knüpfer, G. Lange, J. Appl. Phys. 64 (1988) 1405–1412.
[10] H.H. Rüter, H. von Seggern, R. Reininger, V. Saile, Phys. Rev. Lett. 65 (1990) 2438–2441.
[11] L. Wöhler, G. Rodewald, Z. Anorg. Allg. Chem. 61 (1909) 54–90.
[12] P. Ehrlich, B. Alt, L. Gentsch, Z. Anorg. Allg. Chem. 283 (1956) 58–73.
[13] P. Ehrlich, H. Görtz, Z. Anorg. Allg. Chem. 288 (1956) 148–155.
[14] P. Ehrlich, H. Kulke, Z. Anorg. Allg. Chem. 288 (1956) 156–170.
[15] B. Tanguy, M. Pezat, C. Fontenit, J. Portier, Comp. Rendus Séc. C 280 (1975) 1019–1020.
[16] H.P. Beck, A. Limmer, Z. Naturforschung 37b (1982) 574–578.
[17] H.P. Beck, A. Limmer, Z. Anorg. Allg. Chem. 502 (1985) 185–190.
[18] O. Reckeweg, F.J. DiSalvo, Z. Naturforschung 65b (2010) 493–498.
[19] O. Reckeweg, J.C. Molstad, S. Levy, C. Hoch, F.J. DiSalvo, Z. Naturforschung 63b (2008) 513–518.
[20] O. Reckeweg, F.J. DiSalvo, Z. Naturforschung 66b (2011) 21–26.
[21] O. Reckeweg, J.C. Moldtstad, S. Levy, F.J. DiSalvo, Z. Naturforschung 62b (2007) 23–27.
[22] O. Reckeweg, F.J. DiSalvo, Z. Naturforschung 66b (2011) 1087–1091.
[23] O. Reckeweg, F.J. DiSalvo, S. Wolf, Th. Schleid, Z. Anorg. Allg. Chem. 640 (2014) 1254–1259.
[24] N. Kunkel, D. Rudolph, A. Meijerink, S. Rommel, R. Weihrich, H. Kohlmann, Th. Schleid, Z. Anorg. Allg. Chem. 641 (2015) 1220–1224.
[25] D. Rudolph, D. Enseling, T. Jüstel, Th. Schleid, Z. Anorg. Allg. Chem. 643 (2017) 1525–1530.
[26] H.A. Höppe, H. Lutz, P. Morys, W. Schnick, A. Seilmeier, J. Phys. Chem. Sol. 61 (2000) 2001–2006.
[27] C. Poesl, W. Schnick, Chem. Mater. 29 (2017) 3778–3784.
[28] A. Meijerink, G. Blasse, J. Lumin. 43 (1989) 283–289.
[29] N. Kunkel, A. Meijerink, H. Kohlmann, Phys. Chem. Chem. Phys. 16 (2014) 4807–4813.
[30] R. Hahn, N. Kunkel, C. Hein, R. Kautenburger, H. Kohlmann, RSC Adv. 5 (2015) 9722–9728.
[31] N. Kunkel, A.D. Sontakke, S. Kohaut, B. Viana, P. Dorenbos, J. Phys. Chem. C 120 (2016) 29414–29422.
[32] N. Kunkel, A. Meijerink, H. Kohlmann, Inorg. Chem. 53 (2014) 4800–4802.
[33] N. Kunkel, H. Kohlmann, J. Phys. Chem. C 120 (2016) 10506–10511.
[34] C. Pflug, A. Franz, H. Kohlmann, J. Solid State Chem. 258 (2018) 391–396.
[35] G.F. Hüttig, Z. Anorg. Allg. Chem. 114 (1920) 161–173.
[36] F. Kubel, H. Bill, H. Hagemann, Z. Anorg. Allg. Chem. 625 (1999) 643–649.
[37] N. Kunkel, H. Kohlmann, A. Sayede, M. Springborg, Inorg. Chem. 50 (2011) 5873–5875.
[38] J.L. Sommerdijk, A. Bril, J. Lumin. 11 (1976) 363–367.
[39] P. Dorenbos, J. Phys. Condens. Matter 15 (2003) 2645–2665.
[40] P.E. Cade, A.M. Stoneham, P.W. Tasker, Phys. Rev. B 30 (1984) 4621–4639.
[41] R.C. Baetzold, Phys. Rev. B 36 (1987) 9182–9190.
[42] R.C. Baetzold, K.S. Song, Phys. Rev. B 48 (1993) 14907–14914.
[43] K. Somaiah, H. Hari Babu, Phys. Status Solidi B 117 (1983) 75–79.
[44] A.J. Maeland, W.D. Lahar, Z. Phys. Chem. 179 (1993) 181–185.
[45] C. Messer, J. Solid State Chem. 2 (1970) 144–145.
[46] H. Hagemann, H. Bill, J.M. Rey, F. Kubel, L. Calame, D. Lovy, J. Phys. Chem. C 119 (2015) 141–147.
[47] T. Penhouet, H. Hagemann, F. Kubel, A. Rief, J. Chem. Crystallogr. 37 (2007) 469–472.
[48] N. Kunkel, A. Meijerink, M. Springborg, H. Kohlmann, J. Mater. Chem. C 2 (2014) 4799–4804.
[49] S.H.M. Poort, A. Meijerink, G. Blasse, J. Phys. Chem. Solids 58 (1997) 1451–1456.
[50] A.H. Reshak, M.Y. Shalaginov, Y. Saeed, I.V. Kityk, S. Auluck, J. Phys. Chem. B 115 (2011) 2836–2841.
[51] R.D. Shannon, R.C. Shannon, O. Medenbach, R.X. Fischer, J. Phys. Chem. Ref. Data 31 (2002) 931–970.
[52] B. Henderson, G.F. Imbusch, Optical Spectroscopy of Inorganic Solids, Clarendon Press: Oxford, U.K., 1989.
[53] C.-K. Duan, M.F. Reid, Z. Wang, Phys. Lett. A 343 (2005) 474–480.
[54] J.C. Boyer, F. Vetrone, J.A. Capobianco, A. Speghini, M. Bettinelli, J. Phys. Chem. B 108 (2004) 20137–20143.
[55] C.-K. Duan, M.F. Reid, Curr. Appl. Phys. 6 (2006) 348–350.
[56] D. Rudolph, Doctoral Thesis, University of Stuttgart, 2018.
[57] P. Dorenbos, J. Lumin. 104 (2003) 239–260.
[58] C. Ronda, Luminescence, Wiley-VCH, Weinheim, 2008.
[59] T. Kobayashi, S. Mroczkowski, J.O. Owen, L.H. Brixner, J. Lumin. 21 (1980) 247–257.
[60] K. Rajamohan Reddy, K. Annapurna, S. Buddhudu, Mater. Lett. 28 (1996) 489–490.
[61] B. Tanguy, P. Merle, M. Pezat, C. Fouassier, Mater. Res. Bull. 9 (1974) 831–836.
[62] N. Kunkel, T. Wylezich, Z. Anorg. Allg. Chem. (2019), https://doi.org/10.1002/zaac.201800408 (In press).